Journal of Power Sources 183 (2008) 668–673

Contents lists available at ScienceDirect

Journal of Power Sources

journal homepage: www.elsevier.com/locate/jpowsour

Importance of pressure gradient in solid oxide fuel cell electrodes for modeling study

Meng Ni*, Dennis Y.C. Leung, Michael K.H. Leung

Department of Mechanical Engineering, The University of Hong Kong, Pokfulam Road, Hong Kong, PR China

ARTICLE INFO

Article history:
Received 7 April 2008
Received in revised form 2 May 2008
Accepted 2 May 2008
Available online 9 May 2008

Keywords:
SOFC
Methane steam reforming (MSR)
Water gas shift (WGS)
Porous media
Mass transfer
Electrochemical model

ABSTRACT

The pressure gradients in the electrodes of a solid oxide fuel cell (SOFC) are frequently neglected without any justification in calculating the concentration overpotentials of the SOFC electrodes in modeling studies. In this short communication, a comparative study has been conducted to study the effect of pressure gradients on mass transfer and the resulting concentration overpotentials of an SOFC running on methane (CH_4) fuel. It is found that the pressure gradients in both anode and cathode are significant in the fuel cell electrochemical activities. Neglecting the anode pressure gradient in the calculation can lead to underestimation of the concentration overpotential by about 20% at a typical current density of 5000 A m^{-2} and at a temperature of 1073 K. The deviation can be even larger at a higher temperature. At the cathode, neglecting the pressure gradient can result in overestimation of the concentration overpotential by about 10% under typical working conditions.

1. Introduction

Solid oxide fuel cells (SOFCs) promise efficient electricity generation for stationary applications at an efficiency greater than conventional heat engines [1]. Operating at high temperatures (1073–1273 K), SOFCs have a number of advantages over low-temperature fuel cells such as: (1) electrochemical reactions are fast at high temperatures, leading to low activation overpotential and effective use of low-cost catalyst, such as Ni; (2) the electrolyte at a high temperature has a high ion conductivity, thus the ohmic overpotential of the electrolyte can be minimized; (3) high operating temperature enables direct internal reforming of hydrocarbon fuels in SOFCs, thus SOFCs can utilize a variety of fuels, including CO, which is an unwanted poisonous gas for low-temperature fuel cells; (4) waste heat from SOFCs is of high quality and can be recovered by using a bottoming cycle to increase the system efficiency [2].

However, the high operating temperature limits the choice of materials used for SOFCs. The adverse thermal expansion mismatch of the SOFC components and catalyst sintering may also occur at a high temperature. In order to resolve these material and long-term stability problems, great research efforts have been done to reduce the operating temperature of SOFCs to about 773 K [3]. The reduction in operating temperature decreases the electrode activity and electrolyte ionic conductivity, which in turn leads to lower SOFC performance. Accordingly, the development of electrode with high electrochemical activity and electrolyte with high ionic conductivity are desired. An alternative way to reduce the considerable ohmic overpotential is to fabricate thin film electrolyte. Presently, thin electrolyte with a thickness of only 10 μm can be fabricated by a number of methods, such as tape casting and co-firing [4], sol–gel method [5], and polymer assisted combustion method [6]. In order to provide a strong mechanical support for the SOFC, either the anode or the cathode must be thick enough (≥500 μm). Anode support is the most favorable configuration for SOFCs as the cell performance is generally much better than the cathode-supported SOFC [7–9].

In an anode-supported SOFC, accurate calculation of the gas composition at the anode–electrolyte interface is extremely important as it can strongly affect not only the concentration overpotentials but also the activation overpotentials, due to the dependence of the electrochemical reaction kinetics on the concentrations of reactant and product species [8,10]. In particular, accurate calculation of the concentration overpotential is very important for design optimization of an anode-supported SOFC working at high fuel utilizations, as "a small error in the concentration overpotential calculation may cause a dramatic change to its design performance" [11].

The concentration overpotentials of an SOFC can be modeled by Fick model (FM), Dusty Gas model (DGM) or Stefan-Maxwell

* Corresponding author. Tel.: +852 2859 2811; fax: +852 2858 5415.
E-mail address: memni@graduate.hku.hk (M. Ni).

0378-7753/$ – see front matter © 2008 Elsevier B.V. All rights reserved.
doi:10.1016/j.jpowsour.2008.05.013

model (SMM). Among the three models, DGM can predict the mass transfer in porous SOFC electrodes more accurately as it takes into account Knudsen diffusion phenomena and eliminates the assumption of equal-molar counter diffusion in FM, which becomes invalid if the molecular weights of the diffusing gas species differ considerably [11]. In addition to diffusion, another possible mechanism governing the multi-component mass transfer is permeation, which is driven by pressure gradient inside the porous electrodes. This pressure gradient can be produced by non-equal-molar diffusion of gas species [12], or different molar consumption/production of reactants/products. For example, in the porous cathode, O_2 gas is consumed without any gas product; thus, a pressure gradient will be established across the porous cathode layer. In the porous anode of a H_2 fed SOFC, the pressure gradient occurs due to different diffusion rates of H_2 and H_2O. When hydrocarbon fuels, such as methane, are used in SOFCs, internal methane steam reforming (MSR) and water gas shift (WGS) reactions can be initiated in the porous anode, which in turn can lead to a non-uniform distribution of pressure in the SOFC anode. However, most studies in literature totally neglected the effect of pressure gradient on concentration overpotentials of SOFC electrodes without any justification even for SOFC running on hydrocarbon fuels with MSR and WGS [7,10,13–46]. Therefore, it is still not clear how and to what extent the existence of pressure gradient affects the concentration overpotential calculation. This short communication is purposely designed to study the effect of pressure gradients on SOFC concentration overpotentials. In this study, methane is considered as a model hydrocarbon fuel for the SOFC.

2. The model

2.1. Concentration overpotentials

Concentration overpotential reflects the resistance of the porous electrode structure to the transport of reacting species to and products from the triple phase boundary (TPB) at the electrode–electrolyte interface, where the electrochemical reactions take place. For SOFCs using pure H_2 fuel, or when H_2 is the only electrochemically reacting fuel, the concentration overpotential at the anode ($\eta_{conc,a}$) and cathode ($\eta_{conc,c}$) can be expressed as

$$\eta_{conc,a} = \frac{RT}{2F} \ln\left(\frac{P^S_{H_2} P^I_{H_2O}}{P^I_{H_2} P^S_{H_2O}}\right) \quad (1)$$

$$\eta_{conc,c} = \frac{RT}{4F} \ln\left(\frac{P^S_{O_2}}{P^I_{O_2}}\right) \quad (2)$$

where R is the universal gas constant; T is the working temperature; F is the Faraday constant; P_i is the partial pressure of species i (i refers to H_2, H_2O, and O_2 for respective pressure); the superscripts S and I indicate the partial pressure at the electrode surface and the electrode–electrolyte interface, respectively. The surface partial pressures ($P^S_{H_2}$, $P^S_{H_2O}$, $P^S_{O_2}$) are given as known input parameters while the interface partial pressures ($P^I_{H_2}$, $P^I_{H_2O}$, and $P^I_{O_2}$) need to be determined by analyzing the mass transfer inside the porous electrodes.

2.2. Multi-component mass transfer in porous electrodes

The mass transfer in porous SOFC electrodes is governed by two mechanisms: (1) diffusion due to concentration gradients of reacting species and (2) permeation driven by pressure gradient. As the mean pore size of SOFC electrode is comparable to the mean free path of the reacting gases, the Knudsen diffusion effect must be considered. DGM takes into account the molecular diffusion, Knudsen diffusion, and permeation for the multi-component mass transfer in the porous electrodes,

$$\frac{N_i}{D^{eff}_{i,k}} + \sum_{j=1,j\neq i}^{n} \frac{y_j N_i - y_i N_j}{D^{eff}_{ij}} = -\frac{1}{RT}\left[P\frac{dy_i}{dx} + y_i\frac{dP}{dx}\left(1 + \frac{B_0 P}{D^{eff}_{i,k}\mu}\right)\right] \quad (3)$$

where N_i, y_i, and $D^{eff}_{i,k}$ are the flux, molar fraction and effective Knudsen diffusion coefficient of species i; D^{eff}_{ij} is the effective binary diffusion coefficient of species i and j; P is pressure; x is the depth measured from electrode surface; μ is the viscosity of the gas mixtures; and B_0 is the permeability of the porous electrode, which can be calculated by the Kozeny-Carman relationship [47],

$$B_0 = \frac{\varepsilon^3}{72\xi(1-\varepsilon)^2}(2r_p)^2 \quad (4)$$

The effective diffusion coefficients ($D^{eff}_{i,k}$, D^{eff}_{ij}) can be determined by the following equations [48],

$$D^{eff}_{i,k} = \frac{\varepsilon}{\xi}\frac{4r_p}{3}\sqrt{\frac{8RT}{\pi M_i}} \quad (5)$$

$$D^{eff}_{ij} = 0.00133\frac{\varepsilon}{\xi}\left(\frac{1}{M_i} + \frac{1}{M_j}\right)^{0.5}\frac{T^{1.5}}{P\sigma^2_{i,j}\Omega_D} \quad (6)$$

where ε, ξ, and r_p are the porosity, tortuosity and mean pore radius of the electrodes; and M_i is the molecular weight of species i; Ω_D is a dimensionless diffusion collision integral and $\sigma_{i,j}$ is the mean characteristic length of species i and j. The values of Ω_D and $\sigma_{i,j}$ can be obtained from literature [49].

The pressure gradient (dP/dx) can be evaluated with a method developed by Zhu and Kee [50]:

$$\frac{dP}{dx} = \frac{-\sum_{i=1}^{n}(N_i/D^{eff}_{i,k})}{(1/RT) + (B_0 P/RT\mu)\sum_{i=1}^{n}(y_i/D^{eff}_{i,k})} \quad (7)$$

Eq. (17) comes from summation of Eq. (3) over all species i.

If the effect of pressure gradient is neglected, then Eq. (3) is simplified to

$$\frac{N_i}{D^{eff}_{i,k}} + \sum_{j=1,j\neq i}^{n} \frac{y_j N_i - y_i N_j}{D^{eff}_{ij}} = -\frac{1}{RT}P\frac{dy_i}{dx} \quad (8)$$

which is commonly used in literature.

2.3. Methane steam reforming and water gas shift reactions

In practice, an SOFC can be fed with H_2 or hydrocarbon fuels. Here, CH_4 is used as a model hydrocarbon fuel for SOFC. The major chemical reactions involved are methane steam reforming (MSR) and water gas shift reactions,

$$CH_4 + H_2O \leftrightarrow CO + 3H_2 \quad (9)$$

$$CO + H_2O \leftrightarrow CO_2 + H_2 \quad (10)$$

It should be mentioned that both H_2 and CO could be electrochemically oxidized at the TPB. However, it is legitimate to neglect the electrochemical oxidation of CO because: (1) the rate of CO electrochemical oxidation is much lower than the electrochemical oxidation of H_2 and (2) the rate of CO electrochemical oxidation is much lower than the chemical oxidation of CO by WGS [51,52].

The reaction rates (mol m^{-3} s^{-1}) of MSR (R_{MSR}) and WGS (R_{WGS}) in the porous anode can be, respectively, written as [53].

$$R_{MSR} = k^+_{MSR} p_{CH_4} p_{H_2O} - k^-_{MSR} p_{CO} (p_{H_2})^3 \quad (11)$$

and

$$R_{WGS} = k^{+}_{WGS} p_{CO} p_{H_2O} - k^{-}_{WGS} p_{CO_2} p_{H_2} \quad (12)$$

where k are rate constants for MSR and WGS (mol m^{-3} Pa^{-2} s^{-1}); the superscripts + and − refer to the forward and backward reactions, respectively.

In a steady state, the transport of each participating component is determined by the local conservation of mass:

$$\frac{dN_{CH_4}}{dx} = -R_{MSR} \quad (13)$$

$$\frac{dN_{H_2O}}{dx} = -R_{MSR} - R_{WGS} \quad (14)$$

$$\frac{dN_{CO}}{dx} = R_{MSR} - R_{WGS} \quad (15)$$

$$\frac{dN_{H_2}}{dx} = 3R_{MSR} + R_{WGS} \quad (16)$$

$$\frac{dN_{CO_2}}{dx} = R_{WGS} \quad (17)$$

where N_i is the flux of species i (mol m^{-2} s^{-1}) and x is the depth measured from electrode surface.

The governing equations (Eqs. (3), (7), (8) and (11)–(17)) can be solved numerically to obtain the partial pressure of gas/product species at the electrode–electrolyte interface. It should be mentioned that in the calculation procedure, Eq. (3) should be applied to all transporting species to model the transport of all gas species. The finite difference method can be used to discretize the governing equations, which can be solved with an iterative scheme.

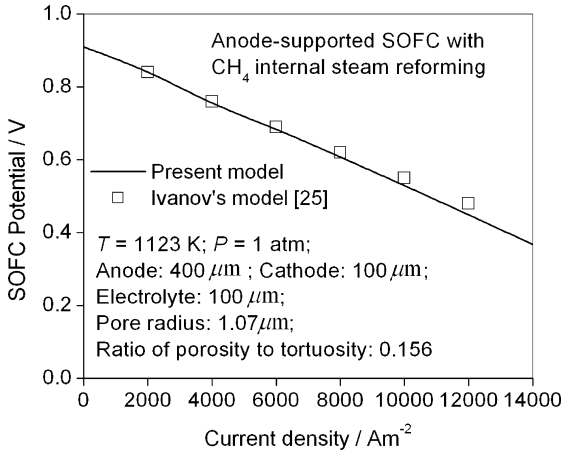

Fig. 1. Comparison between the present simulation results and literature data [25] for model validation.

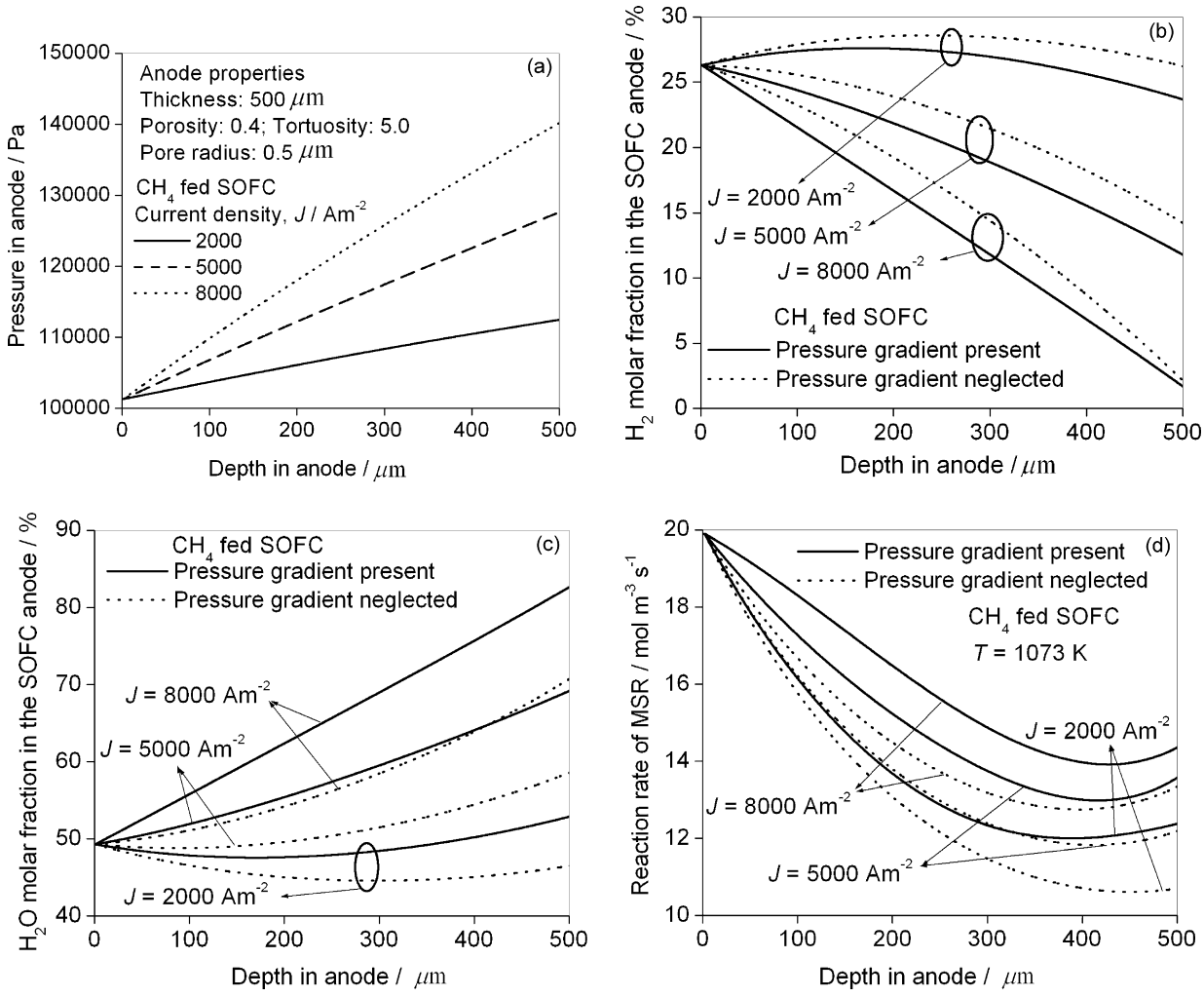

Fig. 2. Distributions of pressure, gas composition and MSR reaction rate in the anode of an SOFC running on CH_4 with internal MSR and WGS: (a) pressure; (b) molar fraction of H_2; (c) molar fraction of H_2O; and (d) reaction rate of MSR.

Table 1
Input parameters used in the mathematical model

Parameter	Value
Temperature, T (K)	1073
Pressure at the electrode surface, P (atm)	1.0
Fuel composition (molar fraction) at the anode inlet [25,52]	
CH_4	17.1%
CO	2.9%
H_2O	49.3%
H_2	26.3%
CO_2	4.4%
Electrode porosity	0.4
Electrode tortuosity	5.0
Electrode pore radius (μm)	0.5
Anode thickness, d_a (μm)	500
Cathode thickness, d_c (μm)	50

After obtaining the interfacial partial pressures of the reacting gas species, the concentration overpotentials of the anode and cathode can thus be calculated by Eqs. (1) and (2), respectively.

3. Results and discussions

The electrochemical model presented in Section 2 was validated in the previous studies [54,55]. A comparison between the present simulation results and data from literature is illustrated in Fig. 1. It can be seen that the present results agree well with Ivanov's [25] data, thus the model presented in this paper is reliable for more analyses. In this section, the effect of pressure gradient on the concentration overpotentials is presented and discussed. In the following analyses, two cases are considered: (1) with pressure gradient inside the porous electrodes, and (2) without pressure gradient inside the porous electrodes. The typical values of the model parameters are summarized in Table 1.

3.1. Anode of an SOFC running on CH_4

Fig. 2 shows the pressure, gas composition and MSR reaction rate in the anode of an SOFC running on CH_4 with internal MSR and WGS. The pressure in the anode is found to increase significantly along the anode depth (Fig. 2(a)). This is because (1) the total molar number of the MSR (Eq. (9)) product is twice as many as that of the reactants and (2) the diffusion of H_2 is faster than that of H_2O due to its smaller molecular weight (non-equal-molar diffusion) [12]. As this pressure gradient adversely impedes the transport of H_2, the H_2 molar fraction is found lower than the case of neglecting the pressure gradient (Fig. 2(b)). On the other hand, as the pressure gradient favors the transport of H_2O, the molar fraction of H_2O is larger if the pressure gradient in the anode is considered (Fig. 2(c)). Due to smaller H_2 molar fraction and larger H_2O molar fraction, higher rate of MSR is observed with pressure gradient considered (Fig. 2(d)). The rate of MSR initially decreases with increasing anode depth due to the decreased molar fraction of CH_4 while it tends to increase in a layer near the anode–electrolyte interface where the molar fraction of H_2O is high. This explains why the pressure increases at a slightly smaller rate in deeper layer of the anode (may not be easily observed in Fig. 2(a)). With an increase in current density, the molar fraction of H_2 decreases while the molar fraction of H_2O increases due to the enhanced electrochemical oxidation reaction (Figs. 2(b) and (c)). The reduction in H_2 molar fraction and increase in H_2O molar fraction can increase the rate of MSR reaction (Fig. 2(d)), which in turn increases the pressure gradient in the porous anode (Fig. 2(a)).

When the pressure gradient inside the anode is considered, the anode concentration overpotential is found higher than the case if the pressure inside the anode is assumed to be invariant (Fig. 3(a)). The concentration overpotential is actually the combined effects of mass transfer resistance and direct internal MSR and WGS. At a low current density, the molar fraction of H_2 at the TPB can be higher than that at the anode surface due to H_2 production through MSR and WGS. Therefore, the anode concentration overpotential is found negative at low current density (Fig. 3(a)). More importantly, the difference in concentration overpotential between the two cases is found significant. For example, at a typical current density of 5000 A m^{-2}, the anode concentration overpotential considering the pressure gradient is 0.053 V, while the value is 0.036 V if the pressure gradient in the anode is totally neglected. In addition to current density, fuel utilization is another useful parameter for characterizing the SOFC performance. For an SOFC working under given conditions (temperature, pressure, flow rate, etc.), the fuel utilization is proportional to the current density. Therefore, the above analyses on current density also reveal the fact that high fuel utilization can cause high concentration overpotential.

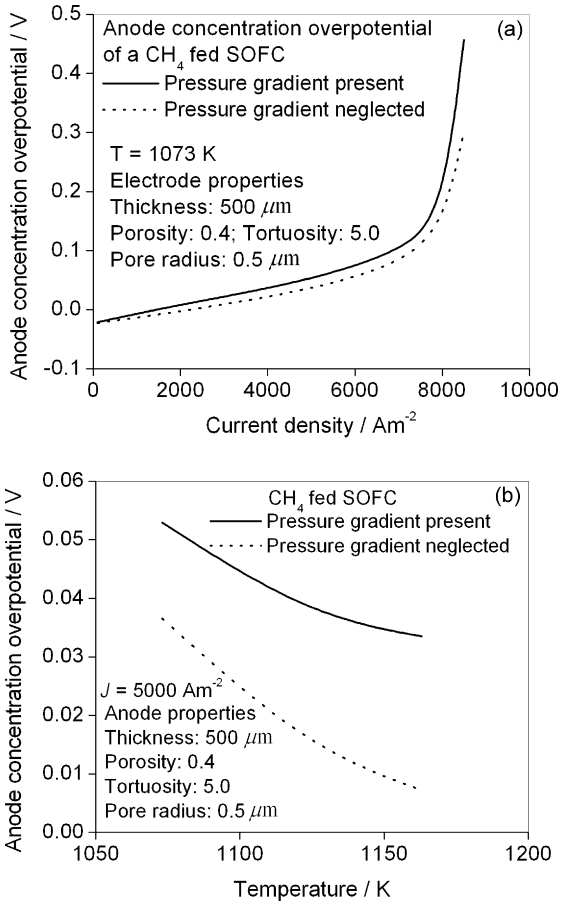

Fig. 3. Effect of pressure gradient on predicting the anode concentration overpotentials of an SOFC running on CH_4: (a) varying current density; and (b) varying temperature.

Fig. 3(b) shows the effect of temperature on the anode concentration overpotentials at a typical current density of 5000 A m^{-2}. For both cases, the anode concentration overpotentials are found to decrease with increasing temperature. This is different from our previous analysis on H_2 fed SOFC, in which the concentration overpotential is found to increase with increasing temperature [8]. When CH_4 is used as a fuel for SOFC, higher temperature favors MSR and WGS, which contribute to more H_2 production inside the porous anode. This in turn increases the H_2 molar fraction and thus leads to lower anode concentration overpotential. In addition, the

difference in concentration overpotential between the two cases becomes more significant at higher temperature (Fig. 3(b)). Since MSR is favored at elevated temperature, the pressure gradient is higher, which in turn leads to more significant effect on anode concentration overpotential.

It should be mentioned that the present study does not include energy equation and assumes uniform temperature distribution along the depth of porous anode. Actually, the endothermic nature of the MSR can lower the temperature of the porous anode and the transporting gas species, which in turn can reduce the rate of MSR for H_2 production. As a result, the pressure gradient can be less significant and the molar fraction of H_2 can be lower. However, based on previous analysis on temperature distribution in the porous anode of SOFC running on methane, the temperature variation in the anode depth is much less than 10 °C [52,56]. Thus, the endothermic nature of MSR only has very small effect on distributions of pressure gradient and gas composition along the anode depth. Nevertheless, the endothermic MSR can cause considerable temperature variation along the fuel flow channel because of large variation in gas composition along the channel [52]. Therefore, in 2D or 3D models, heat transfer model should be included to account for the effect of reaction heat.

From the above analyses, it can be seen that the difference between the two cases is significant in the typical range of current density, especially at a high temperature. Neglecting the effect of pressure gradient can underestimate the concentration overpotential by about 20% at a typical current density of 5000 A m^{-2} (the anode concentration overpotential starts from a negative value). It is thus recommended that the pressure gradient should be included in modeling the anode concentration overpotential of an SOFC running on hydrocarbon fuels.

3.2. Cathode of an SOFC

In this section, the mass transfer and concentration overpotential of the cathode are investigated. Different from the anode, no chemical reactions are involved in the cathode. Taking air as the oxidant, the pressure gradient in the cathode can be expressed as,

$$\frac{dP_c}{dx} = \frac{-((N_{O_2}/D^{eff}_{O_2,k}) - (N_{N_2}/D^{eff}_{N_2,k}))}{((1/RT) + (B_0P_c/RT\mu))((y_{O_2}/D^{eff}_{O_2,k}) + (y_{N_2}/D^{eff}_{N_2,k}))} \quad (18)$$

It is noted that N_{O_2} is equal to $J/4F$ throughout the cathode layer while N_{N_2} is equal to zero. Considering that there is small difference in molecular weights between of O_2 and N_2, $D^{eff}_{N_2,k}$ can be approximated by $D^{eff}_{O_2,k}$. Assuming constant viscosity (μ) in the porous cathode, Eq. (18) can be re-organized to

$$\frac{dP_c}{dx} = \frac{-(N_{O_2}/D^{eff}_{O_2,k})}{(1/RT) + (B_0P_c/RT\mu D^{eff}_{O_2,k})} \quad (19)$$

In Eq. (19), only P_c is a function of cathode depth x, while all other parameters are independent of x. With the boundary condition

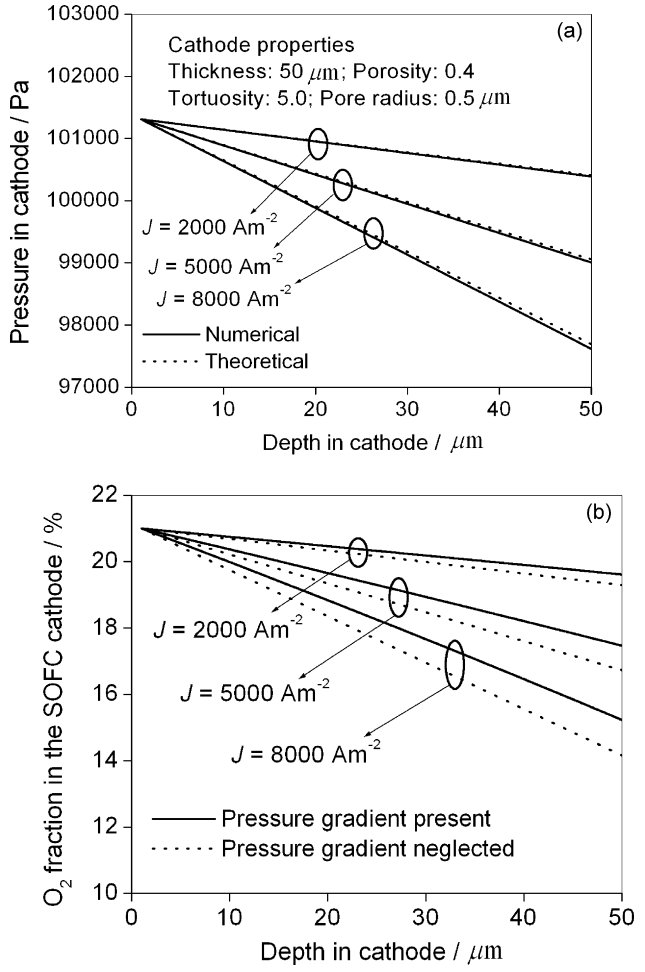

Fig. 4. Distributions of pressure and O_2 molar fraction in the SOFC cathode: (a) pressure; and (b) O_2 molar fraction.

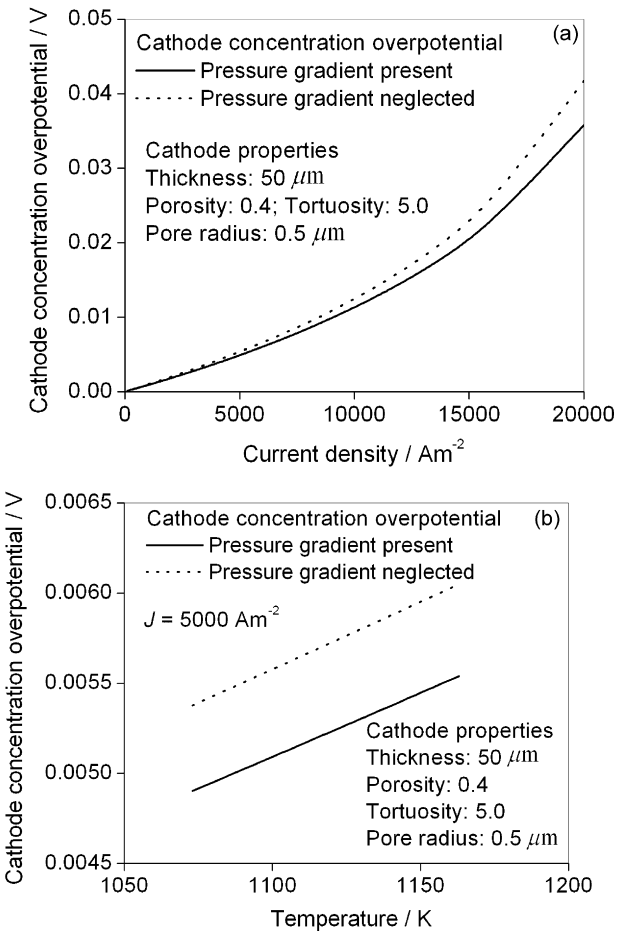

Fig. 5. Effect of pressure gradient on predicting the concentration overpotentials of the SOFC cathode: (a) varying current density; and (b) varying temperature.

of $P_c\big|_{x=0} = P^S = 101310.0\,\text{Pa}$, the analytical solution of the above pressure equation can be derived as

$$P_c = \frac{D^{\text{eff}}_{O_2,k} RT\mu}{B_0}\left[\sqrt{\left(\frac{1}{RT}+\frac{B_0 P^S_c}{D^{\text{eff}}_{O_2,k} RT\mu}\right)^2 - \frac{2B_0 N_{O_2} x}{(D^{\text{eff}}_{O_2,k})^2 RT\mu}} - \frac{1}{RT}\right] \quad (20)$$

With Eq. (20), the pressure distribution in the porous cathode can be analytically calculated without any numerical techniques.

Fig. 4(a) shows the distribution of pressure in the SOFC cathode, calculated by numerical method (DGM) and theoretical solutions (Eq. (20)). It is found that the pressure distribution calculated by the theoretical method (Eq. (20)) agrees very well with that by numerical method (DGM). Thus, the theoretical solution developed in this paper is useful to calculate the pressure distribution quickly and accurately. As expected, the pressure decreases along the cathode depth and the pressure gradient increases with increasing current density due to electrochemical reduction of O_2 at the TPB. Obviously, this pressure gradient is beneficial for O_2 permeation, leading to higher O_2 partial pressure in the porous cathode (Fig. 4(b)) and lower concentration overpotentials (Fig. 5(a)). The difference between the two cases is also considerable. For example, at a typical current density of 5000 A m^{-2}, the cathode concentration overpotential considering pressure gradient is about 0.0049 V, while it is 0.0054 V (10% difference) for the case with the pressure gradient neglected (Fig. 5(a)). Different from the anode, the cathode concentration overpotential increases with increasing temperature (Fig. 5(b)). This is because of lower gas density at higher temperature (Eq. (2)), despite the fact that the effective diffusion coefficients increase with increasing temperature (Eqs. (5) and (6)). In addition, the difference between the two cases is found independent of the operating temperature.

4. Conclusions

A comparative study has been conducted to study the importance of pressure gradient in modeling of SOFC concentration overpotentials. It is found that the pressure gradient in the porous anode of an SOFC running on CH_4 is significant. This pressure gradient impedes the transport of H_2 to the TPB but facilitates transport of H_2O from the TPB to the outer layer of the anode. As a result, neglecting this pressure gradient can underestimate the concentration overpotential by about 20% under typical working conditions. This underestimation would become more serious at a higher temperature. It is thus concluded that the pressure gradient in the porous anode of an SOFC running on hydrocarbon fuels with internal reforming must be considered. At the cathode, neglecting the pressure gradient can overestimate the concentration overpotential by about 10% under typical working conditions.

Acknowledgements

The authors would like to thank the financial support from the CRCG of the University of Hong Kong. The authors also would like to thank Professor S.H. Chan (Nanyang Technological University, Singapore), Professor A.K. Demin (Institute of High Temperature Electrochemistry, Russia), and Professor G.Y. Meng (University of Science and Technology of China, P.R. China) for their valuable discussions and suggestions in SOFC research.

References

[1] S.C. Singhal, K. Kendall, High Temperature Solid Oxide Fuel Cells: Fundamentals, Design, and Applications, Elsevier, Oxford; New York, 2003.
[2] W. Jamsak, S. Assabumrungrat, P.L. Douglas, E. Croiset, N. Laosiripojana, R. Suwanwarangkul, S. Charojrochkul, J. Power Sources 174 (2007) 191–198.
[3] T. Ishihara, J. Tabuchi, S. Ishikawa, J. Yan, M. Enoki, H. Matsumoto, Solid State Ionics 177 (2006) 1949–1953.
[4] H. Moon, S.D. Kim, S.H. Hyun, H.S. Kim, Int. J. Hydrogen Energy 33 (2008) 1758–1768.
[5] H.F. Lin, C.S. Ding, K. Sato, Y. Tsutai, H. Ohtaki, M. Iguchi, C. Wada, T. Hashida, Mater. Sci. Eng. B 148 (2008) 73–76.
[6] C.R. Jiang, J.J. Ma, X.Q. Liu, G.Y. Meng, J. Power Sources 165 (2007) 134–137.
[7] S.H. Chan, K.A. Khor, Z.T. Xia, J. Power Sources 93 (2001) 130–140.
[8] M. Ni, M.K.H. Leung, D.Y.C. Leung, Energy Convers. Manage. 48 (2007) 1525–1535.
[9] M. Ni, M.K.H. Leung, D.Y.C. Leung, J. Power Sources 163 (2006) 460–466.
[10] P. Costamagna, A. Selimovic, M.D. Borghi, G. Agnew, Chem. Eng. J. 102 (2004) 61–69.
[11] R. Suwanwarangkul, E. Croiset, M.W. Fowler, P.L. Douglas, E. Entchev, M.A. Douglas, J. Power Sources 122 (2003) 9–18.
[12] V.H. Schmidt, C.L. Tsai, J. Power Sources 180 (2008) 253–264.
[13] D. Sanchez, R. Chacartegui, A. Munoz, T. Sanchez, J. Power Sources 160 (2006) 1074–1087.
[14] D. Sanchez, R. Chacartegui, A. Munoz, T. Sanchez, Int. J. Hydrogen Energy 33 (2008) 1834–1844.
[15] S.H. Chan, Z.T. Xia, J. Appl. Electrochem. 32 (2002) 339–347.
[16] P. Aguiar, D. Chadwick, L. Kershenbaum, Chem. Eng. Sci. 57 (2002) 1665–1677.
[17] E. Hernandez-Pacheco, D. Singh, P.N. Hutton, N. Patel, M.D. Mann, J. Power Sources 138 (2004) 174–186.
[18] P. Aguiar, C.S. Adjiman, N.P. Brandon, J. Power Sources 138 (2004) 120–136.
[19] E. Hernandez-Pacheco, M.D. Mann, P.N. Hutton, D. Singh, K.E. Martin, Int. J. Hydrogen Energy 30 (2005) 1221–1233.
[20] K.D. Panopoulos, L.E. Fryda, J. Karl, S. Poulou, E. Kakaras, J. Power Sources 159 (2006) 570–585.
[21] M.M. Hussain, X. Li, I. Dincer, Int. J. Energy Res. 29 (2005) 1083–1101.
[22] M.M. Hussain, X. Li, I. Dincer, J. Power Sources 161 (2006) 1012–1022.
[23] M.M. Hussain, X. Li, I. Dincer, Int. J. Thermal Sci. 46 (2007) 56–58.
[24] T. Aloui, Kamel Halouani, Appl. Therm. Eng. 27 (2007) 731–737.
[25] P. Ivanov, Electrochim. Acta 52 (2007) 3921–3928.
[26] Y. Patcharavorachot, A. Arpornwichanop, A. Chuachuensuk, J. Power Sources 177 (2008) 254–261.
[27] K. Nikooyeh, A.A. Jeje, J.M. Hill, J. Power Sources 171 (2007) 601–609.
[28] Y.X. Shi, N.S. Cai, C. Li, C. Bao, E. Croiset, J.Q. Qian, Q. Hu, S.R. Wang, J. Power Sources 172 (2007) 235–245.
[29] J.X. Jia, A. Abudula, L.M. Wei, R.Q. Jiang, S.Q. Shen, J. Power Sources 171 (2007) 696–705.
[30] J.X. Jia, R.Q. Jiang, S.Q. Shen, A. Abudula, AIChE J. 54 (2008) 554–564.
[31] D. Bhattacharyya, R. Rengaswamy, C. Finnerty, Chem. Eng. Sci. 62 (2007) 4250–4267.
[32] S. Campanari, P. Iora, J. Power Sources 132 (2004) 113–126.
[33] P. Nehter, J. Power Sources 157 (2006) 325–334.
[34] P. Costamagna, K. Honegger, J. Electrochem. Soc. 145 (1998) 3995–4007.
[35] B. Morel, J. Laurencin, Y. Bultel, F. Lefebvre-Joud, J. Electrochem. Soc. 152 (2005) A1382–A1389.
[36] J.M. Klein, Y. Bultel, S. Georges, M. Pons, Chem. Eng. Sci. 62 (2007) 1636–1649.
[37] J.M. Klein, Y. Bultel, M. Pons, P. Ozil, J. Fuel Cell Sci. Technol. 4 (2007) 425–434.
[38] P.G. Bavarsad, Int. J. Hydrogen Energy 32 (2007) 4591–4599.
[39] J.C. Ordonez, S. Chen, J.V.C. Vargas, F.G. Dias, J.E.F.C. Gardolinski, D. Vlassov, Int. J. Energy Res. 31 (2007) 1337–1357.
[40] C. Wang, M.H. Nehrir, IEEE Trans. Energy Convers. 22 (2007) 887–897.
[41] C. Bao, N.S. Cai, AIChE J. 53 (2007) 2968–2979.
[42] A.V. Akkaya, Int. J. Energy Res. 31 (2007) 79–98.
[43] J. Deseure, Y. Bultel, L. Dessemond, E. Siebert, P. Ozil, J. Appl. Electrochem. 37 (2007) 129–136.
[44] D.S. Monder, K. Nandakumar, K.T. Chung, J. Power Sources 162 (2006) 400–414.
[45] A. Abbaspour, K. Nandakumar, J.L. Luo, K.T. Chuang, J. Power Sources 161 (2006) 965–970.
[46] K. Nishida, T. Takagi, S. Kinoshita, JSME Int. J. Series B 47 (2004) 786–794.
[47] M. Ni, M.K.H. Leung, D.Y.C. Leung, Electrochim. Acta 52 (2007) 6707–6718.
[48] M. Ni, M.K.H. Leung, D.Y.C. Leung, Chem. Eng. Technol. 29 (2006) 636–642.
[49] R.C. Reid, J.M. Prausnitz, B.E. Poling, The Properties of Gases & Liquids, fourth Edition, McGraw-Hill Book Company, New York, 1987.
[50] H.Y. Zhu, R.J. Kee, J. Power Sources 117 (2003) 61–74.
[51] Y. Matsuzaki, I. Yasuda, J. Electrochem. Soc. 147 (2000) 1630–1635.
[52] V.M. Janardhanan, O. Deutschmann, Chem. Eng. Sci. 63 (2007) 5473–5486.
[53] W. Lehnert, J. Meusinger, F. Thom, J. Power Sources 87 (2000) 57–63.
[54] M. Ni, D.Y.C. Leung, M.K.H. Leung, Electrochemical modeling and parametric study of methane fed solid oxide fuel cell performance, Energy Convers. Manage., submitted for publication.
[55] M. Ni, D.Y.C. Leung, M.K.H. Leung, Modeling of methane fed solid oxide fuel cells: comparison between proton conducting electrolyte and oxygen ion conducting electrolyte, J. Power Sources 183 (2008) 133–142.
[56] B.A. Haberman, J.B. Young, Int. J. Heat Mass Transfer 47 (2004) 3617–3629.